Laboratory demonstration and numerical simulations of the Phase-Induced Amplitude Apodization

Raphael Galicher

Subaru Telescope, 650 N. A'ohoku Place, Hilo, 96720 HI, USA[1]

raphael.galicher@ens.fr

Olivier Guyon

Subaru Telescope, 650 N. A'ohoku Place, Hilo, 96720 HI, USA

guyon@naoj.org

Stephen Ridgway

National Optical Astronomical Observatories

ridgway@noao.org

Hiroshi Suto

Subaru Telescope, 650 N. A'ohoku Place, Hilo, 96720 HI, USA

Masashi Otsubo

Subaru Telescope,Japan

1. Current Phase-Induced Amplitude Apodization instrument

The first prototype of the Phase-Induce Amplitude Apodization (PIAA) is composed of two aspheric lenses. It has been built to validate the following points :

- The computing algorithm produces correct optics shapes.
- apodization of a collimated beam without loss of light or angular resolution.
- verification of the off-axis aberrations.

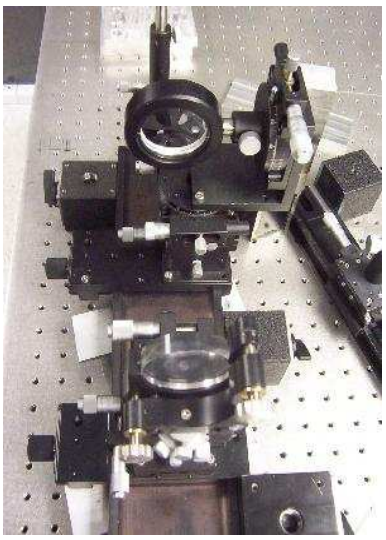

Fig. 1.— *PIAA prototype composed of two aspheric plastic lenses.*

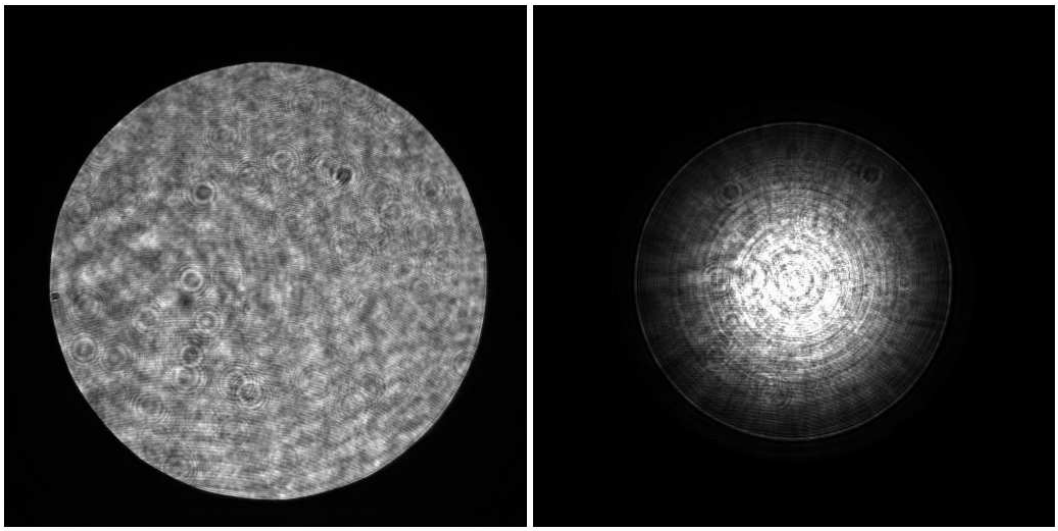

Fig. 2.— *Pupil images without (left) and with (right) PIAA.*

2. Apodization of the pupil

The PIAA optics produce an apodized collimated beam (right in figure 2) from a non-apodized collimated beam (left in figure 2). A shearing interferometer shows the beam is well

[1]École Normale Supérieure, 45 rue d'Ulm, Paris, 75005, France.

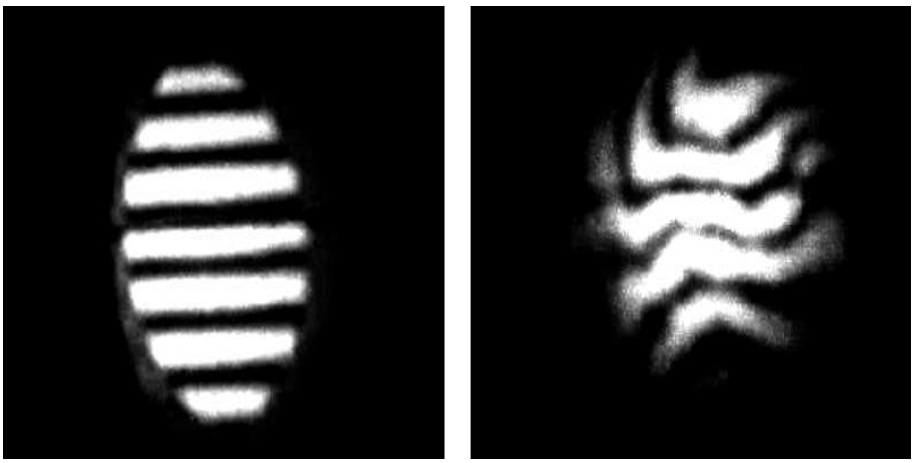

Fig. 3.— *Images of the screen of a shearing interferometer used with the beam without (left) and with (right) the PIAA.*

collimated without (left in figure 3) and with (right in figure 3) PIAA. To illustrate how the PIAA changes the geometrical distribution of the light in the pupil plane, we put a striped mask in this plane and took two images without (left in figure 4) and with (right in figure 4) PIAA. Making circular averages, we obtain the radial profiles of the light intensity in the pupil plane with and without PIAA (figure 5). The bright rings observed in the apodized pupil are due to polishing defects of the lenses (diamond turning). However, the geometrical distribution of the light in the pupil plane is changed and the PIAA produces an apodized collimated beam without loss of flux or angular resolution.

3. On-axis source Point Spread Function

The radial profiles of the Point Spread Function (PSF) with (dashed line) and without (continuous line) PIAA are shown in figure 6. Polishing defects on the two aspheric lenses introduce phase errors in the pupil plane, which explains the bad PSF the current prototype produces. To know the exact impact of these defects, we simulated a PIAA providing the same apodized function but without any phase errors. The obtained PSF is much better than the one obtained with the PIAA prototype. Moreover, the simulated PIAA strongly attenuates the first Airy ring. Indeed, the brightness of the first bright ring is $1.63\,10^{-2}$ at $1.64\frac{\lambda}{d}$ without PIAA. At the same distance, $1.64\frac{\lambda}{d}$, the simulated PIAA yields a brightness of $2.70\,10^{-4}$ instead of $5.50\,10^{-2}$ with the PIAA prototype. The simulations confirm that the polishing defects on the lenses are the main limitation of the PIAA prototype and they

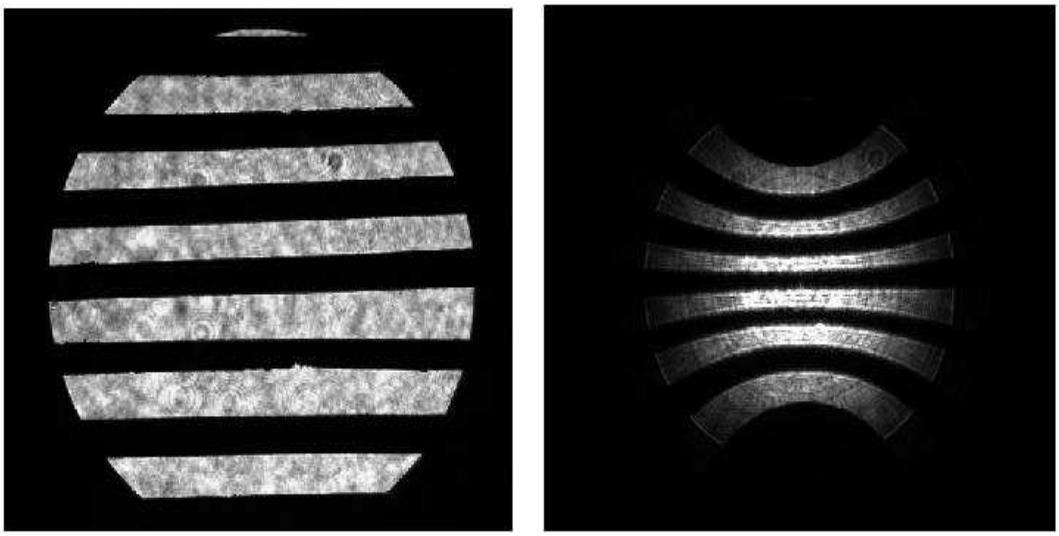

Fig. 4.— *Pupil images of a striped mask without (left) and with (right) the PIAA.*

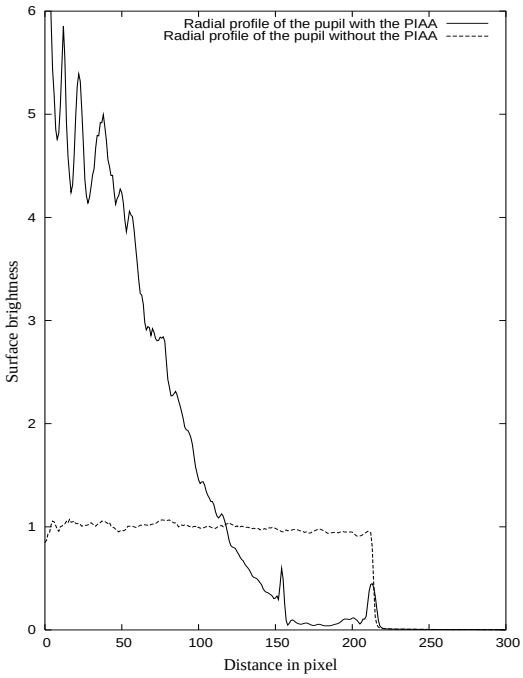

Fig. 5.— *Pupil radial profiles of the light intensity without and with the PIAA.*

also prove that with a deformable mirror we could correct phase errors and obtain a good extinction of the first bright Airy ring.

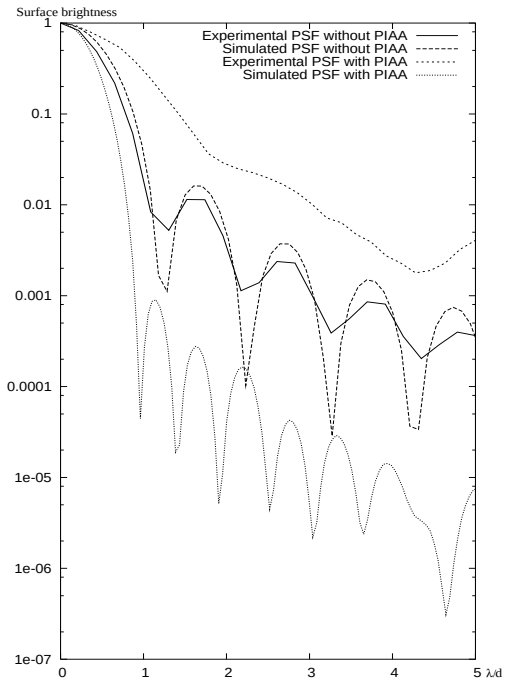

Fig. 6.— *Pupil radial profiles of the light intensity without and with the PIAA.*

4. Off-axis source Point Spread Functions

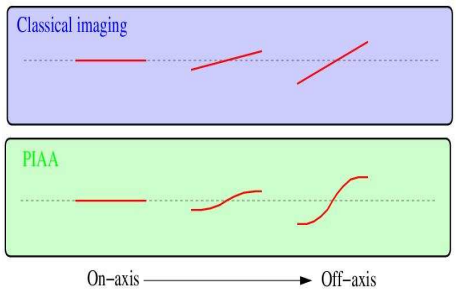

Fig. 7.— *Phase of on-axis (left) and off-axis (middle and right) sources without (top) and with (bottom) the PIAA.*

For an off-axis source, the PSF provided by the PIAA is not only a translation of the on-axis source PSF. Indeed, the PIAA redistributes both the amplitude and the phase of the incoming pupil plane. Through the PIAA, an off-axis source produces a distorted wavefront (not only a tilt as seen in figure 7). As a consequence, the PSF of an off-axis source is complex

and presents a characteristic shape shown in figure 8. We compare experimental (left column) and computed (middle column) PSFs of off-axis sources. Even if some differences, due to polishing errors in the lenses, can be noticed, the general shape of the PSFs and the plate scale are in agreement with our 2D simulations.

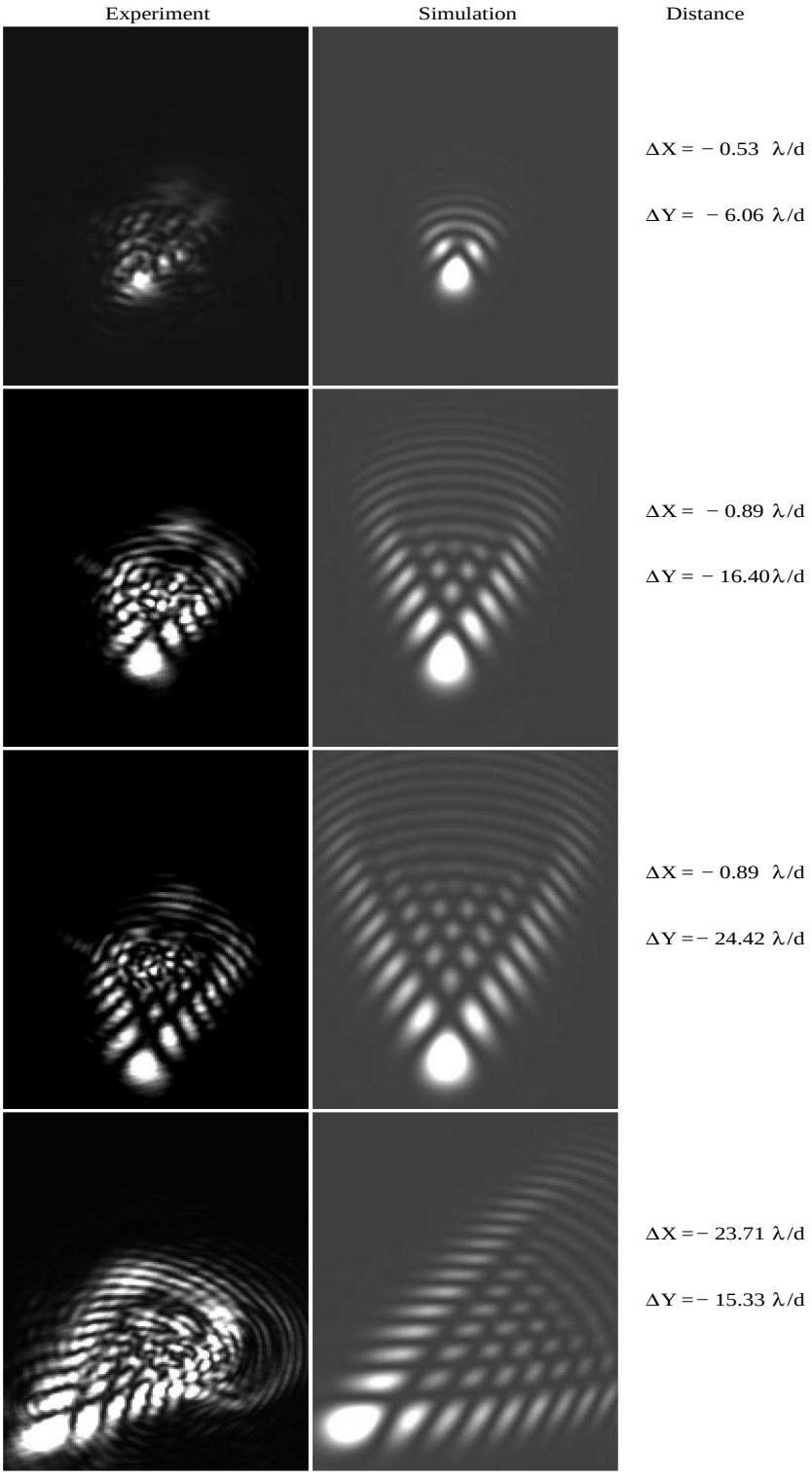

Fig. 8.— *Experimental (left column) and simulated (middle column) off-axis PSFs with the PIAA.*